

**METALLIC ASTEROID DYNAMOS DRIVEN BY CRUSTAL DELAMINATION.** F. Nimmo<sup>1</sup>, J.A. Neufeld<sup>2,3,4</sup>, J.F.J. Bryson<sup>2</sup> <sup>1</sup>Dept. Earth and Planetary Sciences, University of California Santa Cruz, Santa Cruz, CA 95064, USA ([fnimmo@es.ucsc.edu](mailto:fnimmo@es.ucsc.edu)), <sup>2</sup>Dept. Earth Sciences, <sup>3</sup>B.P. Institute <sup>4</sup>Dept. Applied Mathematics & Theoretical Physics, University of Cambridge, Cambridge CB2 3EQ, UK.

**Summary:** Metallic asteroid cores solidifying from the top down may suffer delamination from the base of the solid crust. The resulting buoyancy flux can drive a dynamo which has properties consistent with those inferred from a paleomagnetic study of iron meteorites.

**Introduction:** Metallic asteroids - the cores of planetesimals exposed by a subsequent disruptive impact - are a target of future spacecraft exploration [1]. An important question is whether these bodies developed dynamos and thus might possess remanent magnetic fields. Such dynamos might be driven by either thermal [2,3] or compositional [4,5] convection, with the latter generally being a more efficient process [4]. Here we present an analytical treatment of a novel compositional convection mechanism, and investigate its consequences.

**Observations:** The Steinbach IVA iron meteorite cooled relatively slowly and derived from a parent body which crystallized from the top down [6]. Recent paleomagnetic measurements show that Steinbach recorded a strong (>100 μT), directionally-varying magnetic field [7], presumably of internal origin.

**Model:** The model we propose is sketched in Fig 1. A solidifying iron crust will contain a warm, low-viscosity boundary layer near its base. Because the liquid beneath is less dense, this situation is unstable and will result in delamination [8], whereby solid diapir-like blobs will detach from the crust and sink, forming a growing solid core. The sinking blobs are a source of buoyancy which can drive a dynamo.

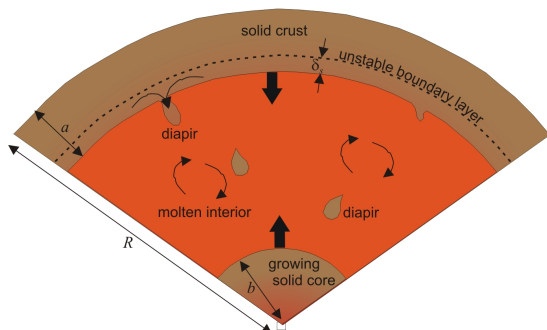


**Figure 1:** Sketch of the situation we envisage, in which a solidifying iron crust undergoes episodic delamination of the warm, low viscosity boundary layer.

**Thermal Evolution:** An initially superheated liquid core will convect vigorously. But the low viscosity of the liquid will rapidly (~100 years) remove the superheat and shut down thermal convection. Thereafter

the rate of crustal growth is controlled by the conductive removal of latent heat, and delamination. The competition between these two effects is captured by the dimensionless ratio  $F'_s/S$ , where  $F'_s$  is the dimensionless solid flux

$$F'_s = \frac{\Delta\rho}{\rho} \frac{1}{2\gamma} \left( \frac{2\lambda}{\gamma} \right)^{4/3} \left( \frac{Ra_s}{7C} \right)^{1/3} \left( 1 - \frac{a}{R} \right)^{1/3}$$

and  $S=L/C_p\Delta T$  is the Stefan number with  $L$  the latent heat,  $C_p$  the specific heat capacity and  $\Delta T$  the temperature contrast between liquid and surface. Here  $\rho$  and  $\Delta\rho$  are the liquid density and solid-liquid density contrast,  $\gamma^{-1}$  is the thickness of the boundary layer relative to the total crust,  $\lambda$  is the Stefan constant,  $Ra_s$  is the buoyancy Rayleigh number of the viscous solid iron and  $C$  is a constant. Note that the solid flux is almost independent of the thickness of the crust ( $a$ ). For nominal parameters  $F'_s/S \ll 1$  so that cooling and latent heat extraction dominate delamination: the situation becomes a standard Stefan problem. Delamination is thus a minor contributor to the thermal evolution, but it controls whether or not a dynamo occurs.

**Nominal Results:** Figure 2 shows the evolution for a 200 km radius metallic asteroid using our nominal parameters. After 25 Myr the top half of the asteroid has solidified, and the top ~30 km of the crust is below the Curie temperature and can thus record a magnetic field.

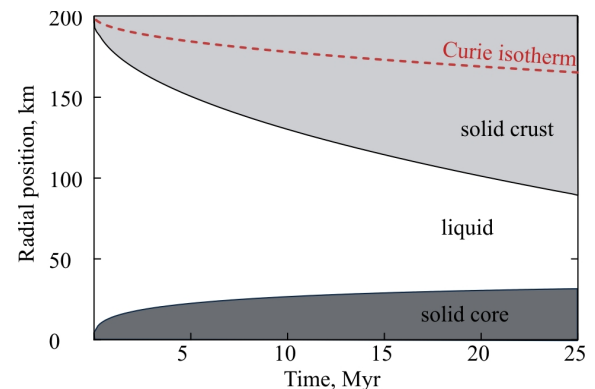


**Figure 2:** Evolution of the solid crust and solid core for our nominal model (body radius 200 km).

**Magnetic Field Evolution:** The solid buoyancy flux due to delamination is given by

$$F_b \approx \frac{4}{3} \pi G \rho (R - a) \left[ \frac{2\gamma\rho\kappa}{R} F'_s \right]$$

Here  $G$  is the gravitational constant,  $R$  the radius of the body,  $a$  the crustal thickness and  $\kappa$  is the thermal diffusivity. The term in square brackets is the dimensional solid mass flux and the  $(R-a)$  term accounts for the reduction in gravity with depth. This buoyancy flux can then be used to calculate the strength of the magnetic field and whether it is expected to be time-variable or not [9,10].

**Nominal results:** Figure 3 shows the evolution of the cooling rate at 800 K in the crust, and the predicted magnetic field strength. The inferred Steinbach cooling rate [6] is reached at about 2 Myr. At this time, the predicted magnetic field strength is about 200  $\mu\text{T}$ , consistent with the inferred lower bound [7]. The local Rossby number exceeds 0.12, implying a multipolar and time-variable field [10], also consistent with the paleomagnetic measurements.

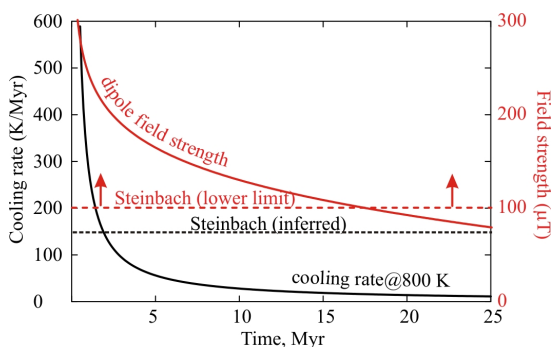


**Figure 3:** Evolution of the cooling rate at 800 K in the solid crust and the predicted magnetic field strength for our nominal model. Observational constraints from [6] and [7] are indicated as dashed horizontal lines.

**Strain history:** The asteroid will contract as it cools and solidifies, potentially leading to compressional features observable at the surface, perhaps similar to those at Mercury or the Moon. Figure 4 shows the evolution of strain and strain rate. The total linear strain is a few percent, at least an order of magnitude larger than the fault-accommodated contraction inferred at Mercury [11]. The strain rate is generally less than  $10^{-16} \text{ s}^{-1}$ , several orders of magnitude lower than strain rates due to plate tectonics on Earth.

**Parameter Values:** Many of the parameters required are uncertain. Parameters of particular importance are the parent body size and the viscosity of solid iron. A body smaller than about 100 km will have a cooling rate that is too large, and a magnetic Reynolds number too low for a dynamo to operate. The solid iron viscosity is poorly known [12], and will control the rate at which delamination happens via  $Ra_s$ . We take a nominal value for solid iron at the melting point

of  $10^{17} \text{ Pa s}$ . Decreasing the viscosity increases the solid flux, which promotes a stronger dynamo but also causes more rapid solid core growth. If the viscosity becomes sufficiently low the crustal growth will be slowed or halted because of efficient delamination.

**Effect of sulphur.** So far we have ignored the effect of sulphur [13]. This reduces the melting point of the liquid and is expelled from the solid, potentially leading to a buoyant layer immediately beneath the crust. The effect of the melting temperature reduction will be to progressively increase the solid iron viscosity with time, thereby reducing the buoyancy flux and shutting the dynamo off earlier. Further work is required to investigate the role of sulphur in more detail.

**Conclusion.** We find that naked iron asteroids can have dynamos driven by compositional, but not by thermal, convection. A solidifying iron crust undergoing delamination gives results which are consistent with measurements of IVA iron meteorites [6,7]. The inferred strain history suggests that compressional features will be observed at the surface of metallic asteroids.

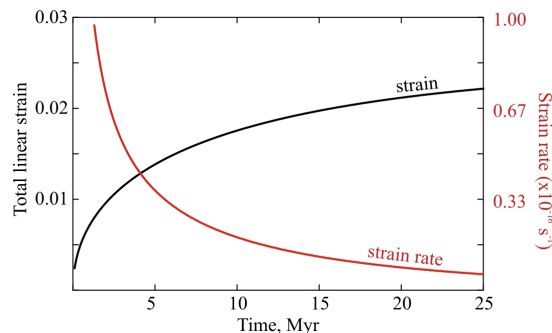


**Figure 4:** Evolution of linear surface strain due to contraction and instantaneous surface strain rate.

**References:** [1] Elkins Tanton & Bell, EPSC2017-384, 2017. [2] Elkins-Tanton et al. EPSL 305, 1-10, 2011. [3] Sterenborg & Crowley, PEPI 214, 53-73, 203. [4] Nimmo GRL 36, L10201, 2009. [5] Scheinberg et al., JGR 121, 2-20, 2016. [6] Yang et al., GCA 72, 3043-3061 (2008). [7] Bryson et al., EPSL 472, 152-163 (2017). [8] Conrad & Molnar GJI 129, 95-112, 1997. [9] Weiss et al. SSR 152 341-390, 2010. [10] Christensen SSR 152, 565-590, 2010. [11] Di Achille et al., Icarus 221, 456-460, 2012. [12] Frost & Ashby, Deformation mechanism maps, Pergamon, Oxford 1982 [13] Chabot, GCA 68, 3607-3618, 2004.